A first-principle analysis on the properties of Mg$_x$Zn$_{1-x}$O alloys

DEPING XIONG[*], XINGUI TANG, WEIREN ZHAO, TIEDONG CHENG, QIUXIANG LIU
School of Physics and Optoelectronic Engineering, Guangdong University of Technology, Guangzhou 510006, China

A first-principle calculation is used to simulate the variation of lattice constant, total energy, and band -gap of hexagonal and cubic Mg$_x$Zn$_{1-x}$O alloys with different Mg composition. The calculated results show the lattice constant *c* and the ratio *c/a* decrease gradually for hexagonal Mg$_x$Zn$_{1-x}$O with Mg composition increasing, the total energy of hexagonal Mg$_x$Zn$_{1-x}$O alloys is lower than, equal to, and larger than that of the cubic one, respectively, the phase transition may occur with Mg composition is 0.79. In addition, the band-gap of hexagonal Mg$_x$Zn$_{1-x}$O has a bowing parameter of 0.38eV and 0.51eV for ordered and random structure.

1. Introduction

Recently, ZnO has attracted great attention due to its potential applications in UV-lasing optoelectronic devices [1]; a critical step for producing high-efficiency ZnO devices is the fabrication of ZnO-based quantum wells and superlattices, for fabrication of such structures, a common approach is to develop ZnO-based alloys with their band-gap larger or smaller than that of ZnO [2,3]. In 1998, Ohtomo et al. proposed incorporating Mg into ZnO to tune the band-gap of the resulting ternary MgZnO alloys[4]. It is noted that ZnO is hexagonal while MgO has the cubic structure, but the similarity in ionic radii between Mg^{2+}(0.57Å) and Zn^{2+}(0.6Å) allows their replacement in either structure[5], while the Mg composition is within a certain range the hexagonal MgZnO may be available. However, the phase segregation and transition may occur as Mg composition increases [4]. Presently, the applications of these materials have been limited by the difficulties in growing homogeneous materials with low defect level, much properties aren't clear very much until now and a lot of efforts have been made to grow high quality materials. Therefore, it is significant to understand the characteristics of MgZnO alloys more so as to use the materials better in ZnO based devices [6-8].

In this paper, a first-principle calculation is used to simulate the characteristics of MgZnO alloys with different Mg composition in hexagonal and cubic structure, the variation of lattice constant, total energy, and band-gap are calculated, the disorder effect on the characteristics is introduced using a cluster expansion approach.

2. Computational method

The present calculations are carried out using CASTEP code, which is based on density functional theory, using the Perdew-Wang generalized gradient approximation (GGA) as the exchange-correlation functional [9]. In order to simulate the ordered alloys with the hexagonal and cubic structure, we construct 8-atom Mg$_n$Zn$_{4-n}$O$_4$ supercells. The ions are described using an ultrasoft pseudopotential scheme, in which the orbitals of Mg (3s^2), Zn (3d^{10}4s^2), and O (2s^{2}2p^4) are treated as valence electrons [10]. The wave functions are expanded in a plane-wave basis set up to cut-off energy of 450eV [11], where the total energy converges to less than 2×10^{-6}eV/atom. Integrations over the Brillouin zone are performed using a $4 \times 4 \times 4$ grid according to a Monkhorst-Pack set sampling-point scheme.

3. Results and discussion

3.1 Ordered alloys

8-atom supercells of Mg$_n$Zn$_{4-n}$O$_4$ with hexagonal and cubic structures are shown in Fig. 1 (a) and (b); n=0, 1, 2, 3, 4 typifies 0, 0.25, 0.5, 0.75,1 of the Mg composition in Mg$_x$Zn$_{1-x}$O alloys, respectively. At first, the geometries of hexagonal Mg$_n$Zn$_{4-n}$O$_4$ with different n are optimized. After geometry optimization, the lattice constants c and c/a, as well as the total energies are obtained for Mg$_x$Zn$_{1-x}$O alloys, as shown in Table 1.
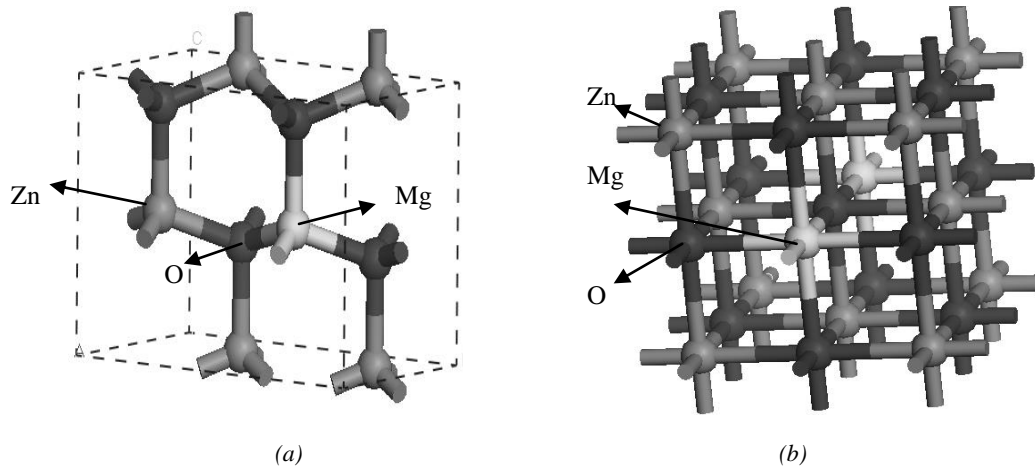
(a)   *(b)*

Fig. 1. The 8-atom hexagonal (a) and cubic (b) Mg$_1$Zn$_3$O$_4$ supercell.

Fig. 2 shows the lattice constants c of hexagonal Mg$_x$Zn$_{1-x}$O as a function of composition x, along with the available experimental results. The present calculations in GGA yield a slight overestimation of the lattice constants in comparison with the experimental values, but the difference between them is within the experimental error range. One can see from Fig. 2 that the introduction of Mg in ZnO leads the lattice constants c and c/a to decrease gradually. The lattice constants of ternary alloys are generally assumed to comply with a simple Vegard's law, i.e., a linear relation of composition x. However, the lattice constants show some amount of deviation from the linear relation in Fig. 2; the curves can be approximated by the following definition:

Where $c(x)$ is the lattice constant c of hexagonal Mg$_x$Zn$_{1-x}$O alloys, c_{MgO} and c_{ZnO} are the lattice constant c of MgO and ZnO, δ_c is the deviation parameter for the lattice constant c, respectively. Using Eq.(1) we best fit the results in Fig. 2 by quadratic polynomial, $\delta_c = -0.14$Å is obtained. Then, the geometries of cubic Mg$_n$Zn$_{4-n}$O$_4$ with different n are optimized; the lattice constants and the total energies are obtained. Fig.3 shows the lattice constants as a function of Mg composition, they gradually decrease with Mg alloying in ZnO, it is because the radii of Mg^{2+} ionic is a little smaller than that of Zn^{2+} ionic. Similarly we fit the results in Fig. 3, $\delta_a =0.0034$Å is obtained for cubic MgZnO. Compared to the hexagonal structure, the lattice constants of cubic MgZnO have very small deviation parameter and comply with the Vegard's law well.

$$c(x) = x \cdot c_{MgO} + (1-x)c_{ZnO} - \delta_c \cdot x \cdot (1-x), \quad (1)$$

Table 1. The calculated lattice constant (Å), total energy (eV) for hexagonal and cubic Mg$_x$Zn$_{1-x}$O alloys.

			0.0	0.25	0.50	0.75	1.0
	This work	$c(x)$	5.249	5.234	5.219	5.190	5.121
		c/a	1.614	1.599	1.585	1.569	1.538
Hexagonal	*Expt. c (x)* [12]	x	0.0	0.05	0.08	0.14	0.23
			5.205	5.196	5.190	5.185	5.177
	Total	Ordered	-8630.776	-7893.504	-7156.213	-6418.898	-5681.565
	energy	Random	-8630.776	-7893.493	-7156.201	-6418.890	-5681.565
Cubic	$a(x)$		4.298	4.292	4.286	4.279	4.272
	Total	Ordered	-8629.535	-7892.734	-7155.899	-6419.030	-5682.121
	energy	Random	-8629.535	-7892.631	-7155.733	-6418.964	-5682.121

In Table 1, it can be seen the total energy of hexagonal $Mg_xZn_{1-x}O$ alloys is lower than, equal to, and larger than that of the cubic one, respectively. Fig.4 plots the total-energy difference between hexagonal and cubic MgZnO dependent on the Mg composition, the phase transition is likely to occur as the Mg composition is larger than 0.69 when the total energy of hexagonal $Mg_xZn_{1-x}O$ is equal to that of cubic $Mg_xZn_{1-x}O$ [13].
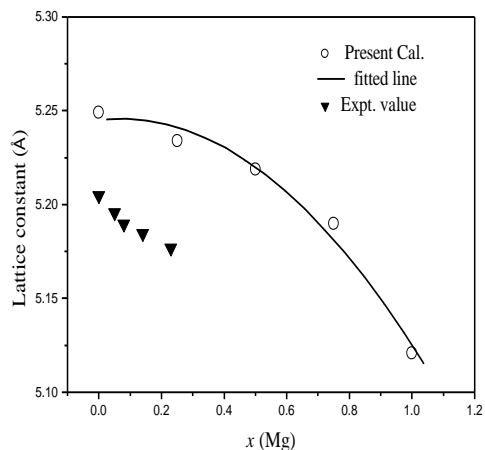

Fig. 2. The lattice constants c of hexagonal $Mg_xZn_{1-x}O$ alloys dependent on the Mg composition.
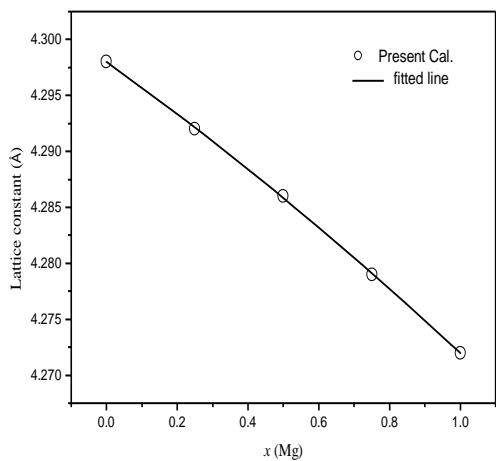

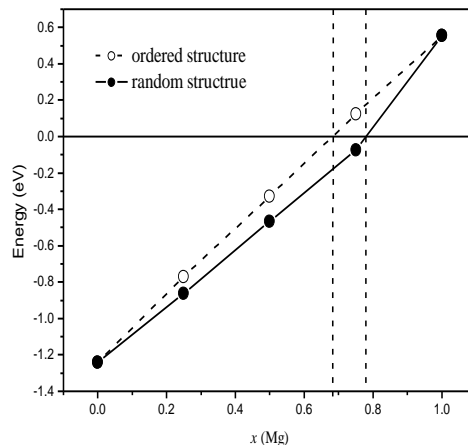*Fig. 3. The lattice constants of cubic $Mg_xZn_{1-x}O$ dependent on the Mg composition.*

Fig. 4. Composition dependence of the calculated total-energy difference between hexagonal and cubic MgZnO.

The calculated band-gaps of hexagonal $Mg_xZn_{1-x}O$ are shown in Table 2 along with available experimental results, they are plotted in Fig.5 for further analysis, the bowing parameters are calculated by the following definition,

$$E_g(x) = x \cdot E_g(MgO) + (1-x) \cdot E_g(ZnO) - b(x) \cdot x \cdot (1-x) \quad (2)$$

Where $E_g(MgO)$ and $E_g(ZnO)$ are the calculated band-gaps of MgO and ZnO, respectively, $E_g(x)$ are the band-gaps of $Mg_xZn_{1-x}O$, $b(x)$ is the band-gap bowing parameter. Substituting the calculated band-gaps in Eq.(2) and obtaining the best fit, a bowing parameter of about 0.38eV is obtained for the hexagonal MgZnO alloys. In this case, the GGA errors can be neglected since only the relatively data is important for bowing parameter calculation [14].
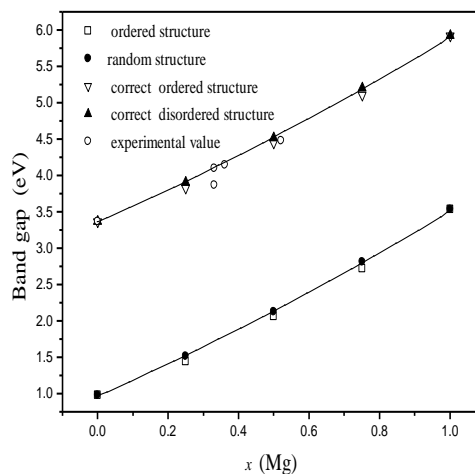

Fig. 5. The calculated band-gaps of hexagonal MgZnO as well as the correct value.

Table 2. Band-gap (eV) variation, bowing parameter (b) in the ordered and random structures, as well as the experimental data for hexagonal MgZnO alloys.

x	0	0.25	0.50	0.75	1.0	b (eV)
Ordered structure	0.980	1.495	2.068	2.724	3.535	0.38
Random structure	0.980	1.521	2.126	2.814	3.535	0.51
x	0	0.33	0.33	0.36	0.51	b(eV)
Expt. value	3.37[15]	3.87 [15]	4.1eV[4]	4.19 [16]	4.45[3]	0.56[17]

Presently there are no experimental band-gap of hexagonal MgO reported, in order to investigate the reliability of the calculated bowing parameter, we also correct the calculated band-gap of hexagonal Mg$_x$Zn$_{1-x}$O simply by a rigid upward of them referred to the experimental value (3.37eV) of hexagonal ZnO, Fig. 5 shows the deviation between experiment and simulation is not large.

3.2. Random alloys

In Mg$_x$Zn$_{1-x}$O alloys, a more probable situation is the alloy may be random. The properties of the random alloy may be simulated by considering the statistical mechanical distributions of the ordered structures. For obtaining such a statistical mechanical properties a cluster expansion method has been used in the past [18, 19], the coefficients of the cluster expansion may be derived by a first-principle calculation of a set of ordered compounds. This method which was first used for binary alloys can be extended to the ternary alloy in the case where the disorder is assumed to occur only on one type of site, say cation as is the case for the Mg$_x$Zn$_{1-x}$O alloys. The problem may further simplify if one truncates the cluster expansion at the level of the nearest neighbor tetrahedron interactions.

Following this idea, any statistical properties $F(x)$ of the random Mg$_x$Zn$_{1-x}$O at a particular composition x can be written as

$$F(x) = \sum_{n=0}^{4} P_n(x) \cdot F_n \qquad (3)$$

$$P_n(x) = \binom{4}{n} x^n (1-x)^{4-n} \qquad (4)$$

Where F_n is the property for each of the five ordered structures, $P_n(x)$ is a statistical weight, representing the probability that the nth short-range ordered structure occurs in the alloy. Using Eq.(4) we have calculated the band-gaps for the random hexagonal Mg$_x$Zn$_{1-x}$O at different Mg composition in Table 2, in Fig. 5 (solid line) the band-gap of the random alloys are depicted and the bowing parameter of 0.51eV is also obtain in Table 2, which is consistent well with the experimental value of 0.56eV in Ref.16 and the calculated value of 0.87eV in

Ref.17. In addition, the total energies of random Mg$_x$Zn$_{1-x}$O are also calculated in Table 1, the difference of the total energy between hexagonal and cubic structure is plotted in Fig. 4 (solid line), as the Mg composition is larger than 0.79 the total energy of hexagonal Mg$_x$Zn$_{1-x}$O is larger than that of cubic Mg$_x$Zn$_{1-x}$O and the phase transition is likely to occur. The calculated result indicates that the structure of the Mg$_x$Zn$_{1-x}$O alloys are hexagonal in large-scale Mg composition, Mg$_x$Zn$_{1-x}$O alloy are suitable for fabricating ZnO-based devices.

4. Conclusion

In summary, the structural and energy properties of Mg$_x$Zn$_{1-x}$O alloys dependent on the Mg composition are calculated using first-principle calculations. As the Mg composition increases, the lattice constants a of the hexagonal Mg$_x$Zn$_{1-x}$O increase from 3.253Å to 3.329Å, while the lattice constants c decrease from 5.249 Å to 5.121Å, which results in the structure gradually deviating from the wurtzite structure; the deviation parameters from Vegard's law are δ_a =0.041Å and δ_c = -0.14Å, respectively. The lattice constants of cubic Mg$_x$Zn$_{1-x}$O diminish gradually with the Mg composition increasing; it is because the atom radius of Mg^{2+} is a little smaller than that of Zn^{2+}, the deviation parameter of δ_a =0.0034Å is obtained. The total energy of hexagonal MgZnO is lower than, equal to, and larger than that of the cubic one, respectively; the phase transition is likely to occur as the Mg composition is larger than 0.79eV. In addition, the band-gaps of hexagonal MgZnO are calculated, a bowing parameter of 0.38eV and 0.51eV is obtained for ordered and random alloys, respectively.

Acknowledgements

Reference

[1] H. Cao, Y. Ling, J. Y. Xu, C. Q. Cao, P. Kumar. Phys. Rev. Lett. **86**, 4524 (2001).

[2] Y. M. Lu, C. X. Wu, Z. P. Wei, J. Cryst Growth. **278**, 299 (2005).

[3] A. Ashrafi, Y. Seqawa, J. Appl. Phys. **104**, 123528 (2008).

[4] A. Ohtomo, M. Kawasaki, T. Koida, K. Masubuchi, H. Koinuma, Appl. Phys. Lett. **72**, 2466-8 (1998).

[5] A. K. Sharma, J. Narayan, J. F. Muth, C. W. Teng, Appl. Phys. Lett. **75**, 3327 (1999).

[6] A. Y. Polyakov, N. B. Smirnov, A. V. Govorkov, J. Electrochem. Soc. **154**, 825 (2007).

[7] Q. Mingxia, Zh. Yinzhu, Y. Zhizhen, J. Phys. D: Appl. Phys. **40**, 3229 (2007).

[8] R. Thangavel, M. Rajagopalan, J. Kumar. Solid State Commun. **137**, 507 (2006).

[9] M. C. Payne, M. P. Teter, D. C. Allan, T. A. Arias, J. D. Joannopoulous, Rev. of Mod. Phys. 64, 1045 (1992).

[10] J. Furthmuller, P .Kachell, F. Bechstedt, G. Kresse, Phys. Rev. B **61**, 4576 (2000).

[11] S. F. Ding, G. H. Fan, S. T. Li, K. Chen, B. Xiao, Phys. B **394**, 127 (2007).

[12] W. Chunxia, L. Youming, S. Dezhen, Chin. J. Semi. 25 (2004) 1258.

[13] X. H. Chen, J. Y. Kang, Semi. Sci.& Tech. **23**, 025008 (2008).

[14] G. L. W. Hart, A. Zunger, Phys. Rev. B **62**(13), 522 (2000).

[15] W. I. Park, G. Yi, H. M. Jang, Appl Phys Lett **79**, 2022 (2001).

[16] W. R. L. Lambrecht, S. Limpijumnong, B. Segall, MRS Internet J. Nitride Semicond. Res. 4S1, G6.8 (1999).

[17] X. F. Fan, H. D. Sun, Z. X. Shen, J. L. Kuo Y. M. Lu, J. Phys.: Conds. Matt. **20**, 235221 (2008).

[18] Bal. K. Agrawal, P. S. Yadav, R. Srivastava, J. Phys.: Conds. Matt **10**, 4597 (1998).

[19] R. Srivastava, P. S. Yadav, S. Agrawal, Savitri Agrawal, Solid State Commun. **118**, 479 (2004).

———————————————

*Corresponding author: depingxiong@gdut.edu.cn, xiongdeping@gmail.com